Size effects in near-ultraviolet Raman spectra of few-nanometer-thick silicon-on-insulator nanofilms

Vladimir Poborchii, Yukinori Morita, Tetsuya Tada, Pavel I. Geshev, Zhandos N. Utegulov, and Alexey Volkov

Citation: Journal of Applied Physics **119**, 154302 (2016); doi: 10.1063/1.4947021
View online: https://doi.org/10.1063/1.4947021
View Table of Contents: http://aip.scitation.org/toc/jap/119/15
Published by the American Institute of Physics

Articles you may be interested in

Raman spectroscopic characterization of germanium-on-insulator nanolayers
Applied Physics Letters **108**, 083107 (2016); 10.1063/1.4942607

Ultraviolet Raman spectra of few nanometer thick silicon-on-insulator nanofilms: Lifetime reduction of confined phonons
Applied Physics Letters **105**, 153112 (2014); 10.1063/1.4898672

Raman spectroscopy of ultrathin strained-silicon-on-insulator: Size effects in strain, elastic, and phonon properties
Applied Physics Letters **106**, 093107 (2015); 10.1063/1.4914031

Raman investigation of strain in Si / SiGe heterostructures: Precise determination of the strain-shift coefficient of Si bands
Journal of Applied Physics **99**, 053512 (2006); 10.1063/1.2178396

Band structure of cavity-type hypersonic phononic crystals fabricated by femtosecond laser-induced two-photon polymerization
Applied Physics Letters **108**, 201901 (2016); 10.1063/1.4949013

Stress measurements in silicon devices through Raman spectroscopy: Bridging the gap between theory and experiment
Journal of Applied Physics **79**, 7148 (1996); 10.1063/1.361485

AIP | Journal of Applied Physics SPECIAL TOPICS LEARN MORE

Size effects in near-ultraviolet Raman spectra of few-nanometer-thick silicon-on-insulator nanofilms

Vladimir Poborchii,[1,a)] Yukinori Morita,[1] Tetsuya Tada,[1] Pavel I. Geshev,[2] Zhandos N. Utegulov,[3] and Alexey Volkov[4]
[1]*Nanoelectronics Research Institute, AIST, Tsukuba Central 5, 1-1-1 Higashi, Tsukuba 305-8565, Japan*
[2]*Institute of Thermophysics of the Russian Academy of Sciences, Lavrentyev Ave. 1, Novosibirsk 630090, Russia and Novosibirsk State University, Pirogova Str. 2, Novosibirsk 630090, Russia*
[3]*Department of Physics, School of Science and Technology, Nazarbayev University, 53 Kabanbai Batyr Ave., Astana 010000, Kazakhstan*
[4]*Interdisciplinary Instrumentation Center, National Laboratory Astana, Nazarbayev University, 53 Kabanbai Batyr Ave., Astana 010000, Kazakhstan*

(Received 1 December 2015; accepted 5 April 2016; published online 18 April 2016)

We have fabricated Si-on-insulator (SOI) layers with a thickness h_1 of a few nanometers and examined them by Raman spectroscopy with 363.8 nm excitation. We have found that phonon and electron confinement play important roles in SOI with $h_1 < 10$ nm. We have confirmed that the first-order longitudinal optical phonon Raman band displays size-induced major homogeneous broadening due to phonon lifetime reduction as well as minor inhomogeneous broadening due to wave vector relaxation (WVR), both kinds of broadening being independent of temperature. Due to WVR, transverse acoustic (TA) phonons become Raman-active and give rise to a broad band in the range of 100–200 cm^{-1}. Another broad band appeared at 200–400 cm^{-1} in the spectrum of SOI is attributed to the superposition of 1st order Raman scattering on longitudinal acoustic phonons and 2nd order scattering on TA phonons. Suppression of resonance-assisted 2-nd order Raman bands in SOI spectra is explained by the electron-confinement-induced direct band gap enlargement compared to bulk Si, which is confirmed by SOI reflection spectra. *Published by AIP Publishing.* [http://dx.doi.org/10.1063/1.4947021]

INTRODUCTION

Si on insulator (SOI) structure, a single-crystal silicon film on an amorphous buried oxide layer (BOX) layer separating the film from Si substrate (Fig. 1), was introduced as a key building block for the next generation microelectronic devices. Due to interesting physical properties, SOI appeared to be a subject of intensive scientific studies in the last decade. High dielectric contrast between Si and SiO_2 as well as high Si Raman efficiency enabled obtaining Si Raman lasing in SOI in the infrared spectral range.[1,2] Another highlighted application of SOI is as an ultra-low-loss waveguide.[3] Interesting nanoscale electronic[4] and mechanical[5–7] properties of SOI also attracted much attention. Studying their electrical, optical, mechanical, and thermal properties is important for both basic science and applications. SOI nanolayers with thickness $h_1 < 10$ nm are considered as important elements in the complementary metal-oxide-semiconductor technology for integrated circuits with enhanced performance such as reduced threshold and applied voltages and increased switching speed.[8] Carrier mobility and thermal conductivity of such thin films are influenced by the electron and phonon confinement, the issue of a special interest. In this work, we study phonon and electron confinement effects in few-nanometer-thick high-quality SOI using Raman and reflection spectroscopy.

SOI nanolayers with a few nanometer thickness weakly interact with visible light while demonstrate strong coupling with near-ultraviolet (near-UV) light.[9–11] Recently, we demonstrated UV Raman and absorption enhancement of a few nanometer thick SOI using a constructive interference in the BOX layer.[9] This attracts interest to SOI as UV photodetectors and even UV-enhanced solar cells for a number of specific applications.[12] Recently, we studied the size effects on the longitudinal optical (LO) phonon Raman band of few-nanometer-thick SOI at the temperature $T \sim 77$ K and observed thickness-inversely-proportional homogeneous LO phonon band broadening that is associated with the phonon lifetime reduction, probably, due to surface disorder.[10] Weaker inhomogeneous band broadening due to phonon confinement and wave vector relaxation (WVR) was also observed. Both band broadening effects together appeared to be much smaller than those suggested by previous results on Raman spectra of Si nanofilms (NFs).[10] That discrepancy was attributed to the difference in NF quality. Indeed, nowadays, the quality of SOI is much better than that of Si NFs years or decades ago. Such high-quality SOI NFs display much sharper Raman bands than bad-quality Si NFs do. This fact is a strong motivation for further studies of SOI size effects in Raman spectra. In this work, we focus on the size effects in the wide-range 1st and 2nd order Raman spectra of SOI.

EXPERIMENTAL

Commercially available initial SOI structures were received from SOITEC. [001]-oriented SOI were located on

[a)]On leave from Ioffe Physico-Technical Institute, St.Petersburg, Russia. Electronic mail: Vladimir.p@aist.go.jp

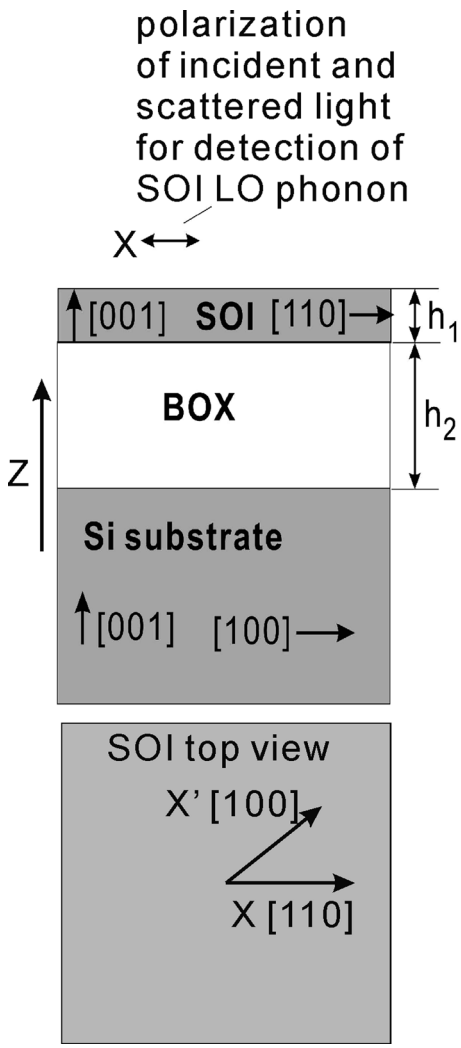

FIG. 1. Schematic view of SOI structure.

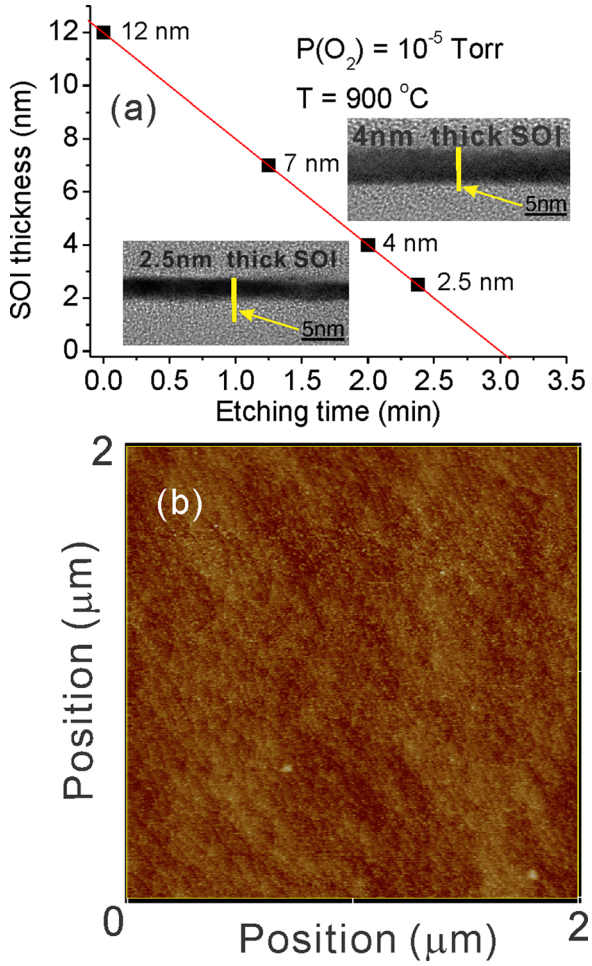

FIG. 2. (a) Dependence of SOI thickness h_1 on the etching time in the oxygen atmosphere at the pressure of $\sim 10^{-5}$ Torr and temperature $\sim 900\,^{\circ}$C. Insets show TEM images of SOI cross-sections with $h_1 \sim 4$ nm and ~ 2.5 nm. (b) AFM topography image of the oxygen-etched surface of the 4 nm thick SOI. Z scale corresponds to 1.68 nm. RMS roughness is ~ 0.1 nm.

the top of a 145 nm BOX ($h_2 = 145$ nm) covering a Si substrate (Fig. 1). Initial thickness of SOI was 70 nm. Then it was reduced using dry etching in the low pressure oxygen atmosphere, where reaction $2Si + O_2 \rightarrow 2SiO\uparrow$ occurred.[13–15] At elevated wafer temperature of 900 °C, migration of Si atoms on the SOI surface was activated, and therefore, atomically flat surface was created. At low oxygen pressure, layer-by-layer etching took place. This method allowed control of h_1 through oxygen pressure and oxidation time with ± 0.5 nm precision. Fig. 2(a) shows dependence of h_1 on the etching time of 12 nm thick SOI. Then, h_1 was checked by the electron microscopy, ellipsometry, and reflection spectroscopy. Insets in Fig. 2(a) demonstrate transmission electron microscopic (TEM) images of ~ 2.5 nm and ~ 4 nm thick SOI. Fig. 2(b) shows an atomic force microscopy (AFM) image of the oxygen-etched surface of $2\,\mu m \times 2\,\mu m$ area of ~ 4 nm thick SOI. Root mean square (RMS) roughness of ~ 0.1 nm was obtained from this image.

Raman measurement was done in the back-scattering geometry with the incident and scattered light directed along the [001] axis of SOI (Z axis in Fig. 1) using a Nanofinder-30 system (Tokyo Instruments Inc.) equipped with a 363.8 nm wavelength Ar^+ laser corresponding to the resonant Raman enhancement and small (10–15 nm) penetration depth of light in silicon.[9–11] In contrast to our previous Raman studies of SOI, where only 1st order allowed LO phonon Raman band was measured, in this work, we also made Raman measurement in a wide 100–1100 cm^{-1} spectral range. The low-frequency instrumental limit was determined by Semrock edge filters used for the suppression of elastically scattered laser light. Wide spectral range measurements were done with the 1800 g/mm diffraction grating, while high-spectral-resolution measurements ($\sim 0.6\,cm^{-1}$) in the Si LO phonon range were done with the Echelle grating working in the 65th order. All measurements were made with the Olympus 0.16 N.A. 4× lens with an incident laser power density $\sim 10\,\mu W/\mu m^2$, which is well below the level of noticeable laser-induced heating of SOI.

The lateral orientation of SOI was different from the orientation of Si substrate (Fig. 1), namely, the [110] axis of SOI was parallel to the [100] axis of Si substrate.[9] This enables making SOI Raman measurement in a polarization configuration XX//[110] with both incident and scattered lights polarized parallel to the SOI [110] axis, which corresponds to the allowed Raman signal of the LO phonon from SOI with no contribution from the Si substrate LO phonon that appears to be in the forbidden XX//[100] configuration.

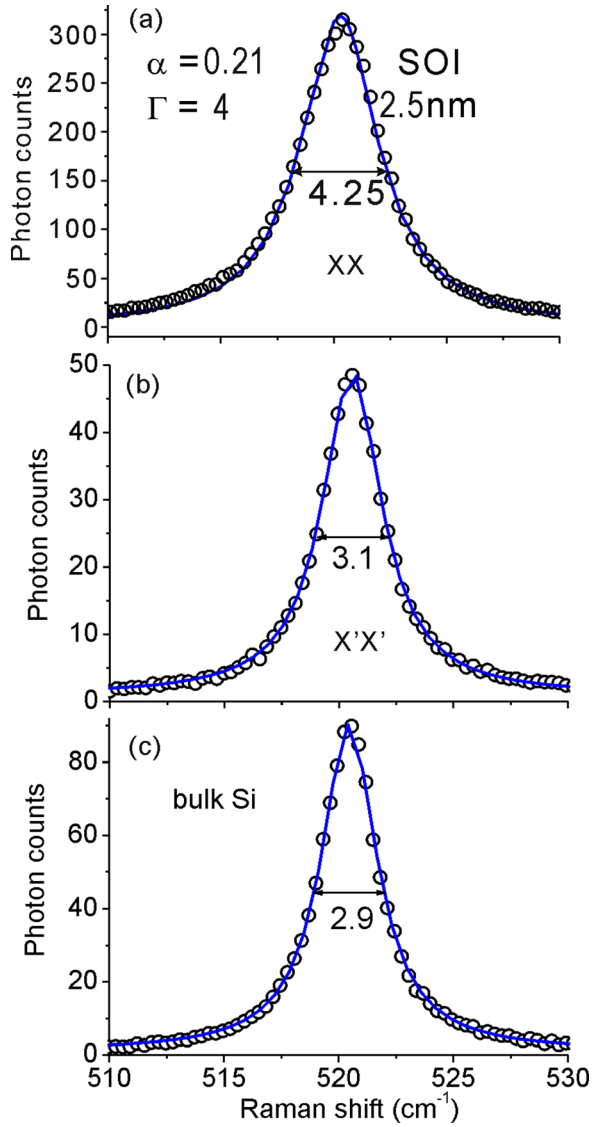

FIG. 3. (a) LO phonon Raman band of ∼2.5 nm thick SOI observed in the *XX*//[110] polarization configuration (circles) and its fitting using RCFAP model (blue curve). (b) LO phonon Raman band of Si substrate with insignificant contribution of ∼2.5 nm SOI band obtained in the $X'X'$//[100] polarization configuration and its Lorentz fitting (blue curve). (c) LO phonon Raman band of bulk Si observed in the *XX*//[110] polarization configuration (circles) and its Lorentz fitting (blue curve).

RESULTS AND DISCUSSION

Fig. 3(a) shows the high-spectral-resolution (∼0.6 cm^{-1}) room-temperature ($T \sim 300$ K) Raman spectrum of ∼2.5 nm thick SOI with the LO phonon Raman band, which is obtained in the *XX*//SOI [110] polarization configuration. The SOI Raman band with the full-width at half-maximum (FWHM) ∼4.25 cm^{-1} is displayed with no contribution from the bulk Si substrate. Fig. 3(b) shows a spectrum of the same sample, which was taken in the forbidden for SOI LO phonon $X'X'$//SOI [100] polarization configuration. The Raman band with FWHM ∼3.1 cm^{-1} originates mainly from the Si substrate, which is allowed in this configuration. It is slightly broader than the bulk Si Raman band with FWHM ∼2.9 cm^{-1} (Fig. 3(c)) due to an insignificant contribution of the SOI band that is not completely suppressed in the $X'X'$//SOI [100] polarization configuration. The vertical axes of all three spectra in Fig. 3 are given in photon counts, and they represent actual intensity ratios of the displayed Raman bands. The SOI band (Fig. 3(a)) is significantly enhanced compared to both substrate (Fig. 3(b)) and bulk Si (Fig. 3(c)) bands due to both reduced reflectance of thin SOI NF and constructive interference of near-UV light in the 145 nm thick BOX.[9]

As one can see, the ∼2.5 nm thick SOI LO phonon experimental Raman band (circles) can be fitted using modified Richter–Campbell–Fauchet (RCF) model (blue curve) taking into account NF thickness-induced phonon lifetime τ reduction.[10,11] We will use abbreviation RCFAP for this modified RCF model. In the classical RCF model,[16] for the dimensionless wave vector q normal to NF, the Raman selection rule $q = 0$ becomes relaxed for a finite-size domain allowing Raman scattering from the non-center Brillouin zone phonons. (This is different from superlattices with crystalline interfaces, where a simple standing-wave model with an effective confinement wave vector q_m can be applied, which results in backfolding of bulk dispersion branches.) The dependence of the Raman signal on the frequency $I_{NF}(\omega)$ can be obtained using integration over the Brillouin zone

$$I_{NF}(\omega) = I_0 \int_0^1 \frac{|C(q)|^2 dq}{(\omega - \omega_0(q))^2 + (\Gamma/2)^2}, \quad (1)$$

where I_0 is proportional to the laser power and $\omega_0(q)$ is the phonon frequency vs. wave vector in the [001] direction[17] perpendicular to NF. In the RCF model,[16] $\Gamma = \Gamma_{bulk}$ is the FWHM of bulk material Raman band. $|C(q)|^2$ is the Fourier coefficient of the confinement function

$$|C(q)|^2 = C_0 \exp[-(qH/\alpha a)^2/2], \quad (2)$$

where C_0 is the constant, $a = 0.543$ nm is the Si lattice parameter, while α is a fitting parameter introduced by Adu *et al.*[18] for nanowires (RCFA model) but it also can be used for NFs, the larger α corresponding to the stronger wave vector q relaxation.

In contrast to RCF and RCFA models, $\Gamma = \Gamma_{bulk}$, whereas in the RCFAP model,[10,11] $\Gamma > \Gamma_{bulk}$ due to the phonon lifetime reduction. RCFAP fitting of the ∼2.5 nm thick SOI LO phonon Raman band (Fig. 3(a)) was done with parameters $\Gamma = 4$ cm^{-1} and $\alpha = 0.21$. This implies homogeneous size-induced band broadening compared to bulk Si $\Delta\Gamma \sim 4 - 2.9 = 1.1$ cm^{-1} and inhomogeneous WVR-induced broadening $\Delta WVR \sim 4.25 - 4 = 0.25$ cm^{-1}. These values appeared to be in very good agreement with corresponding values obtained for ∼2.5 nm thick SOI at the temperature of 77 K.[10] Therefore, both kinds of band broadening are independent of the temperature.

Figure 4 shows the Fourier coefficient of the confinement function corresponding to $h_1 = 2.5$ nm and $\alpha = 0.21$ (black curve). In the same figure, the green line shows bulk Si LO phonon Raman band frequency 520.5 cm^{-1}, while the red curve represents LO phonon dispersion in the [001] direction.[17] As one can see, WVR effect corresponding to $h_1 = 2.5$ nm and $\alpha = 0.21$ is rather weak in contrast, for example, with that reported for ∼4 nm thick silicon on

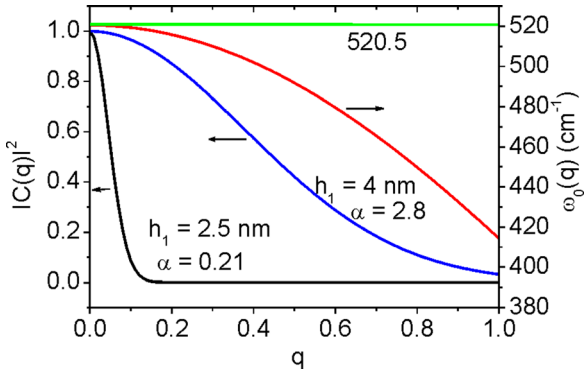

FIG. 4. Fourier coefficient of the confinement function for $h_1 = 2.5$ nm and $\alpha = 0.21$ (black curve) and that for $h_1 = 4$ nm and $\alpha = 2.8$ (blue curve); LO phonon dispersion (red curve) and LO phonon Raman shift (green line).

sapphire (SOS) NF in Ref. 16 requiring $\alpha \sim 2.8$ to fit its Raman band with FWHM $\sim 14\,\mathrm{cm}^{-1}$. The corresponding Fourier coefficient is shown as a blue curve in Fig. 4. Clearly, huge WVR-induced broadening $\Delta WVR \sim 11\,\mathrm{cm}^{-1}$ of SOS NF originates not from the phonon confinement but from the film imperfections and even discontinuities. On the other hand, relatively weak size-induced broadening of the $\sim$2.5 nm SOI LO phonon Raman band demonstrates the high quality of SOI NF studied in this work and, therefore, proves that the observed effects are true size effects but not the effects associated with NF imperfections.

Since Γ is a function of the phonon lifetime τ, namely, $\Gamma = 1/(c\pi\tau)$, where c stands for the speed of light, the homogeneous broadening $\Delta\Gamma \sim 1.1\,\mathrm{cm}^{-1}$ implies LO phonon lifetime reduction from $\sim$3.65 ps in bulk Si ($\Gamma \sim 2.9\,\mathrm{cm}^{-1}$) to $\sim$2.65 ps in $\sim$2.5 nm thick SOI ($\Gamma \sim 4\,\mathrm{cm}^{-1}$). As we proposed earlier,[10] the most probable reason for the τ reduction is the amorphous-oxide-induced surface disorder influencing Si interatomic potential in SOI. The impact of this effect on both optical and acoustic phonons is significant. Recent studies of Si nano-membranes, showing that surface oxidation strongly suppresses thermal conductivity,[19] confirm the strong influence of the surface disorder on Si NF phonon properties.

Figure 5(a) shows Raman spectrum of $\sim$2.5 nm thick SOI in the range from $\sim 100\,\mathrm{cm}^{-1}$ to $1100\,\mathrm{cm}^{-1}$. It is easy to show using the known intensity ratio of LO phonon bands of SOI and Si substrate (Fig. 3) that the substrate just slightly contributes to the Raman spectrum shown in Fig. 5(a). Its contribution is shown as a red curve in Fig. 5(a).

Let us consider features, which are much weaker than the 1st order LO-phonon band at $\sim 520.5\,\mathrm{cm}^{-1}$. One noticeable difference with the spectrum of bulk Si (Fig. 5(b)) can be seen in the range of 100–200 cm^{-1}. An asymmetric broad Raman band, observed in this range of the SOI spectrum, definitely, originates from the 1st order Raman scattering on the transverse acoustic (TA) phonons. Indeed, Si phonon dispersion curves and density of states[17] shown in Fig. 6 display maximal TA phonon density of states in the 100–200 cm^{-1} range. Bulk Si Raman spectra (Fig. 5(b)) display no band in this range since the 1st order acoustic phonon Raman signal

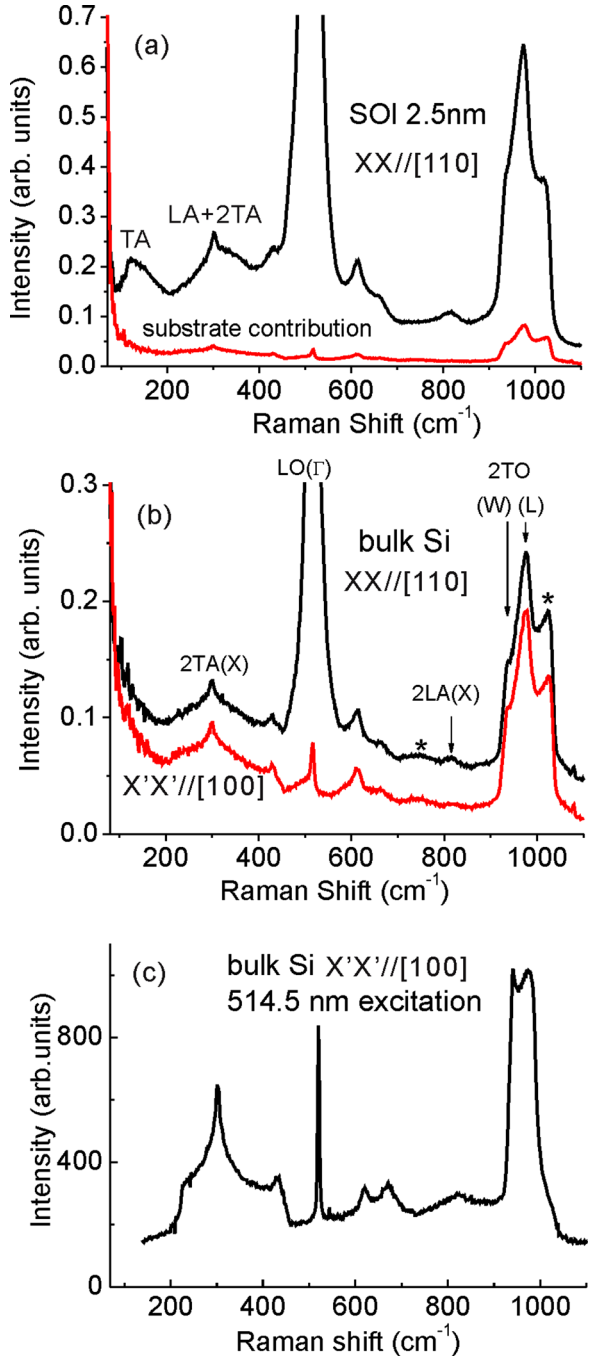

FIG. 5. Raman spectra of $\sim$2.5 nm thick SOI (a) and bulk Si (b) excited by the 363.8 nm laser light and spectrum of bulk Si excited by the 514.5 nm laser light (c). Asterisks show the bulk Si bands displayed due to the resonant Raman scattering at the 363.8 nm excitation.

is forbidden. The acoustic phonon band became Raman-active in SOI due to WVR and, consequently, Raman selection rule $q = 0$ relaxation.

It is important that the WVR approach like in the case of SOI LO phonon appears to be more appropriate than the Brillouin zone folding approach working well for superlattices with crystalline interfaces. Thus, WVR approach works for oxide borders and relatively high phonon frequencies, namely, for optical phonons and acoustic phonons close to maxima of density of states. At the same time, for low-frequency ($<50\,\mathrm{cm}^{-1}$) long-wave acoustic phonons,

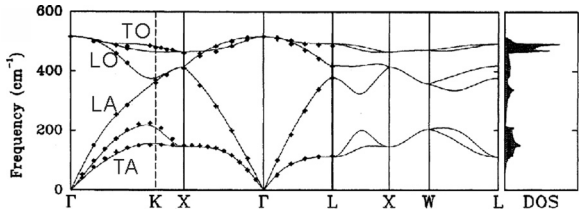

FIG. 6. Calculated Si phonon dispersions and density of states from Ref. 17. Reprinted with permission from P. Giannozzi *et al.*, Phys. Rev. B. **43**, 7231 (1991). Copyright 1991 APS.

backfolding of bulk dispersion branches reasonably works with some corrections even for oxide borders.[20]

In the 200–400 cm^{-1} range, one can see a broad band that is different from a bulk Si sharp feature associated with the 2nd order Raman scattering on TA phonons at the X-point of the Brillouin zone with maximum at ~300 cm^{-1}. Both 2nd order Raman scattering on TA phonons and 1st order scattering on LA phonons can contribute to the broad band at 200–400 cm^{-1}. Indeed, since the $q=0$ rule is relaxed, a broader variety of TA phonon couples can contribute to the 2nd order Raman spectrum of SOI. On the other hand, LA phonon density of states displays a peak at ~350 cm^{-1} corresponding to L-X and W-L valleys (Fig. 6), which can make additional contribution to the 200–400 cm^{-1} Raman band of SOI.

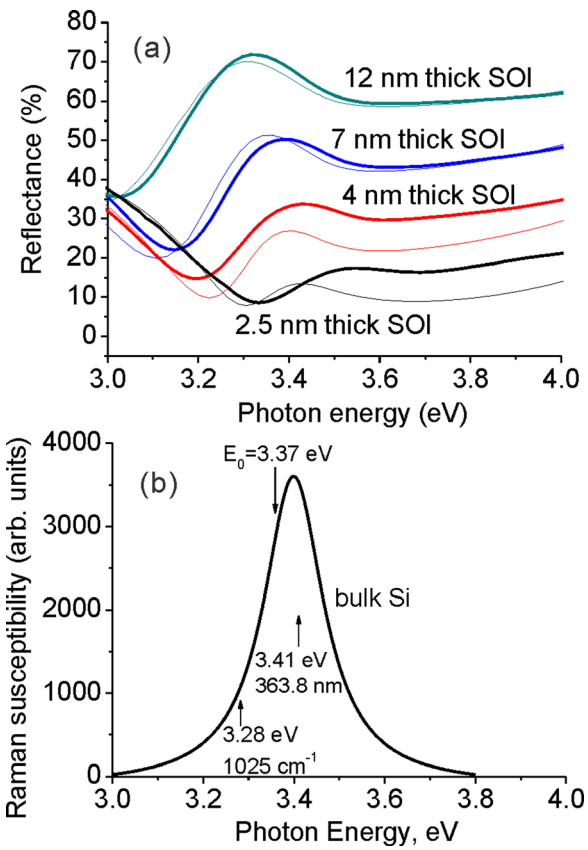

FIG. 7. (a) Experimental (bold lines) and theoretical (thin lines) reflection spectra of SOI with different thicknesses, calculations being made with the optical constants of bulk Si. (b) Spectral dependence of bulk Si Raman susceptibility. Arrows show photon energy of the excitation laser wavelength 363.8 nm, the smallest direct band gap energy E_0, and the energy corresponding to the ~1025 cm^{-1} (~0.13 eV) Raman band.

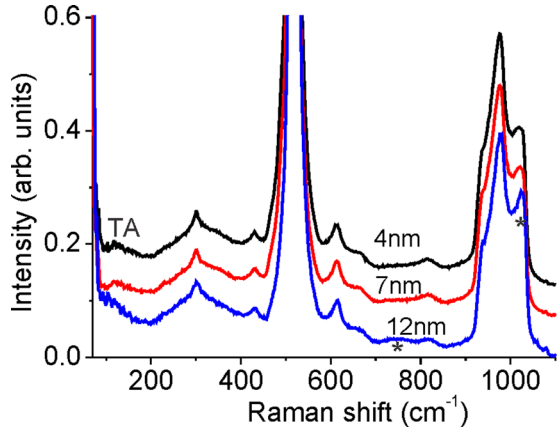

FIG. 8. Raman spectra of SOI with thickness 4, 7, and 12 nm in the *XX*// [110] polarization configuration. Asterisks show the ~12 nm SOI bands displayed due to the resonant Raman scattering at the 363.8 nm excitation.

There are two other noticeable changes in the ~2.5 nm thick SOI Raman spectrum (Fig. 5(a)) compared to the bulk Si one (Fig. 5(b)). Bulk Si displays a band at ~750 cm^{-1}, which is absent in the SOI spectrum, and a band at ~1025 cm^{-1} that is much weaker in the SOI spectrum. These bands marked with asterisks in Fig. 5(b) are displayed in the spectrum of bulk Si due to the resonance of the 363.8 nm (~3.41 eV) light with the direct interband electron transitions in the Γ-L valley of Si Brillouin zone with minimal bandgap $E_0 \sim 3.37$ eV at the Γ point.[21] There are no such bands in the bulk Si Raman spectrum excited with the 514.5 nm laser light (Fig. 5(c)) corresponding to the photon energy ~2.41 eV well below the direct bandgap.

Figure 7(a) demonstrates band gap enlargement in SOI by comparison of experimental reflection spectra with calculated ones using bulk Si optical constants, calculations being made by the method described in Ref. 9. As one can see, in accordance with the quantum size (carrier confinement) effect enlarging energy band gap, experimental reflection peak in the spectrum of 2.5 nm thick SOI displays ~0.1 eV blue shift compared to the peak in the corresponding theoretical spectrum. This value appears to be in good agreement with the direct bandgap enlargement ~0.12 eV in 2.5 nm thick SOI obtained using ellipsometry.[22]

Figure 7(b) shows the spectral dependence of bulk Si Raman susceptibility[23] with linear scale for vertical axis instead of the logarithmic one in the original reference. Arrows show photon energy ~3.41 eV of the excitation laser wavelength 363.8 nm, the smallest direct band gap energy E_0 ~ 3.37 eV, and the energy ~3.28 eV corresponding to the ~1025 cm^{-1} (~0.13 eV) Raman band. The Raman susceptibility curve displays rather sharp resonance centered at ~3.4 eV with FWHM ~0.16 eV. It is clear that the size-induced ~0.1 eV upshift of the resonance in ~2.5 nm thick SOI worsens resonance condition at the ~3.41 eV excitation. Therefore, resonance-associated bulk Si Raman bands at ~750 cm^{-1} and ~1025 cm^{-1} become suppressed in the SOI spectrum.

We have to note that the experimentally observed value ~0.1 eV of the size-induced direct band gap enlargement in ~2.5 nm thick SOI can be determined not only by the carrier

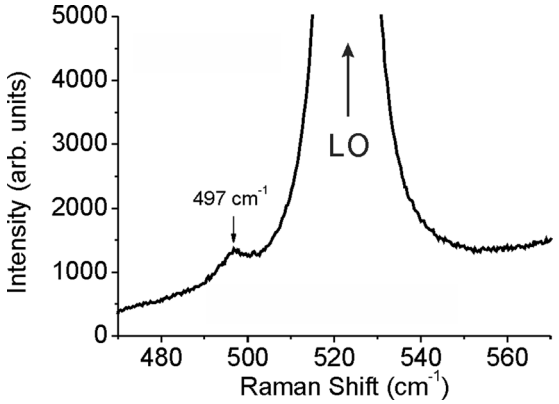

FIG. 9. Raman spectrum of ~2.5 nm thick SOI in the *XX*//[110] polarization configuration in the range near 1st order LO phonon band. The measurement was done at $T \sim 100$ K.

confinement but also by the electron–phonon interaction[22] and, possibly, by some other effects.

Figure 8 shows Raman spectra of ~4, ~7, and ~12 nm thick SOI. The spectrum of ~12 nm thick SOI almost completely coincides with the spectrum of bulk Si shown in Fig. 5(b). At the same time, spectra of ~4 nm and ~7 nm thick SOI display difference with the spectrum of bulk Si. A weak but noticeable 1st order Raman activity of TA phonons in the 100–200 cm^{-1} range can be seen in the spectra of both ~4 nm and ~7 nm thick SOI. Weakening of the ~1025 cm^{-1} band and absence of the ~750 cm^{-1} band due to the Raman resonance detuning are another size-induced effect in the spectra of ~4 nm and ~7 nm thick SOI. However, both size effects look less pronounced in the spectra of ~4 nm and ~7 nm thick SOI than those in the spectrum of ~2.5 nm thick SOI.

One more effect in the Raman spectrum of ~2.5 nm thick SOI can be seen in Fig. 9. This figure shows a high-resolution spectrum, which displays a very weak 497 cm^{-1} Raman band at $T \sim 100$ K, low temperature being used to sharpen the band. The observed Raman shift is close to TO(L) or TA(L) + LA(L) (Fig. 6). However, the assignment of similar band observed in the Raman spectra of Si nanowires to a polycrystalline defect looks more convincing.[24] As the authors of the cited work showed, the band was enhanced after HF etching. A very low intensity of the corresponding band in the ~2.5 nm thick SOI spectrum suggests that the concentration of such defects in our SOI samples is very low.

CONCLUSIONS

We have fabricated high-quality few nanometer thick SOI nanolayers from initial 70 nm thick SOI using dry etching in the low-pressure oxygen atmosphere and studied size effects in their near-UV Raman and reflection spectra. LO phonon Raman band of ~2.5 nm thick SOI displays major homogeneous broadening ~1.1 cm^{-1} due to the phonon lifetime reduction and minor inhomogeneous broadening due to phonon-confinement-induced WVR ~0.25 cm^{-1}. The values of both types of broadening obtained at $T \sim 300$ K coincide with those observed earlier at $T \sim 77$ K and, therefore, suggest that both types of broadening are independent of temperature. Both types of broadening are influenced by the amorphous oxide borders, namely, naturally oxidized surface on the top of SOI and BOX at the bottom of SOI.

In the 100–1100 cm^{-1} range Raman spectrum of ~2.5 nm thick SOI, we observed 1st order TA phonon band at 100–200 cm^{-1} that became Raman active due to WVR. A broad band at 200–400 cm^{-1} was attributed to both 1st order Raman scattering on LA phonons from L-W and X-L valleys of Brillouin zone and 2nd order scattering on TA phonons. Due to direct electron energy bandgap enlargement confirmed by reflection spectra, resonance-assisted bands of bulk Si at ~750 cm^{-1} and ~1025 cm^{-1} appeared to be suppressed in the Raman spectrum of ~2.5 nm thick SOI. As we show, ~4 nm and ~7 nm thick SOI display phonon and electron size effects weaker than those in the spectra of ~2.5 nm thick SOI. At the same time, Raman spectrum of ~12 nm thick SOI was found to nearly coincide with the spectrum of bulk Si suggesting that phonon and electron confinement play important role in SOI with $h_1 < 10$ nm, while no significant phonon size effects in the studied frequency range as well as in the electron spectrum occur in SOI with $h_1 > 10$ nm.

ACKNOWLEDGMENTS

This work was supported by the Nazarbayev University Grant No. SST2015014 and ALCA Project. The work of P. I. Geshev was supported by MES (Russia).

[1]H. Rong, A. Liu, R. Jones, O. Cohen, D. Hak, R. Nicolaescu, A. Fang, and M. Paniccia, Nature **433**, 292 (2005).
[2]H. Rong, R. Jones, A. Liu, O. Cohen, D. Hak, A. Fang, and M. Paniccia, Nature **433**, 725 (2005).
[3]Y. Ma, Y. Zhang, S. Yang, A. Novack, R. Ding, A. E.-J. Lim, G.-Q. Lo, T. Baehr-Jones, and M. Hochberg, Opt. Express **21**, 29374 (2013).
[4]P. Zhang, E. Tevaarwerk, B. N. Park, D. E. Savage, G. K. Celler, I. Knezevic, P. G. Evans, M. A. Eriksson, and M. G. Lagally, Nature **439**, 703 (2006).
[5]F. Liu, M. H. Huang, P. P. Rugheimer, D. E. Savage, and M. G. Lagally, Phys. Rev. Lett. **89**, 136101 (2002).
[6]L. Feng Liu, P. Rugheimer, E. Mateeva, D. E. Savage, and M. G. Lagally, Nature **416**, 498 (2002).
[7]F. Cheynis, E. Bussmann, F. Leroy, T. Passanante, and P. Muller, Phys. Rev. B **84**, 245439 (2011).
[8]X. Tang, N. Reckinger, G. Larrieu, E. Dubois, D. Flandre, J.-P. Raskin, B. Nysten, A. M. Jonas, and V. Bayot, Nanotechnology **19**, 165703 (2008).
[9]V. Poborchii, T. Tada, Y. Morita, S. Migita, T. Kanayama, and P. I. Geshev, J. Appl. Phys. **112**, 074317 (2012).
[10]V. Poborchii, Y. Morita, M. Ishimaru, and T. Tada, Appl. Phys. Lett. **105**, 153112 (2014).
[11]V. Poborchii, M. Hara, Y. Morita, and T. Tada, Appl. Phys. Lett. **106**, 093107 (2015).
[12]V. Poborchii, Y. Morita, T. Tada, P. I. Geshev, Z. Utegulov, and A. Volkov, in *Extended Abstracts of International Conference on Solid State Devices and Materials, SSDM-2015, Sapporo, Japan* (2015), p. 542.
[13]Y. Morita, S. Migita, W. Mizubayashi, and H. Ota, Surf. Sci. **604**, 1432 (2010).
[14]Y. Morita, T. Maeda, H. Ota, W. Mizubayashi, S. O'uchi, M. Masahara, T. Matsukawa, and K. Endo, IEDM Tech. Dig. **2015**, 390.
[15]Y. Morita, S. Migita, N. Taoka, W. Mizubayashi, and H. Ota, in *Extended abstracts of Silicon Nanoelectronics Workshop* (2009), p. 123.
[16]I. H. Campbell and P. M. Fauchet, Solid State Commun. **58**, 739 (1986).
[17]P. Giannozzi, S. de Gironcoli, P. Pavone, and S. Baroni, Phys. Rev. B **43**, 7231 (1991).
[18]K. W. Adu, H. R. Gutierrez, U. J. Kim, G. U. Sumanasekera, and P. C. Eklund, Nano Lett. **5**, 409 (2005).

[19]S. Neogi, J. S. Reparaz, L. F. C. Pereira, B. Graczykowski, M. R. Wagner, M. Sledzinska, A. Shchepetov, M. Prunnila, J. Ahopelto, C. M. Sotomayor-Torres, and D. Donadio, ACS Nano **9**, 3820 (2015).
[20]J. Groenen, F. Poinsotte, A. Zwick, C. M. Sotomayor Torres, M. Prunnila, and J. Ahopelto, Phys. Rev. B **77**, 045420 (2008).
[21]J. B. Renucci, R. N. Tyte, and M. Cardona, Phys. Rev. B **11**, 3885 (1975).
[22]V. K. Kamineni and A. C. Diebold, Appl. Phys. Lett. **99**, 151903 (2011).
[23]A. Compaan, M. C. Lee, and G. J. Trott, Phys. Rev. B **32**, 6731 (1985).
[24]Z. Peng, H. Hu, M. I. B. Utama, L. M. Wong, K. Ghosh, R. Chen, S. Wang, Z. Shen, and Q. Xiong, Nano Lett. **10**, 3940 (2010).